

## **Remediation of Lead-Contaminated Water Using Green Synthesized Iron-Oxide Nanoparticles: Performance and Mechanism**

Authors: Li, Linyi, Haziq, Mohammad Aslam, Ullah, Sajid, Stanikzai, Abdul Ghani, Bibi, Shah Dehrai, et al.

Source: Air, Soil and Water Research, 17(1)

Published By: SAGE Publishing

URL: <https://doi.org/10.1177/11786221241278517>

---

The BioOne Digital Library (<https://bioone.org/>) provides worldwide distribution for more than 580 journals and eBooks from BioOne's community of over 150 nonprofit societies, research institutions, and university presses in the biological, ecological, and environmental sciences. The BioOne Digital Library encompasses the flagship aggregation BioOne Complete (<https://bioone.org/subscribe>), the BioOne Complete Archive (<https://bioone.org/archive>), and the BioOne eBooks program offerings ESA eBook Collection (<https://bioone.org/esa-ebooks>) and CSIRO Publishing BioSelect Collection (<https://bioone.org/csiro-ebooks>).

Your use of this PDF, the BioOne Digital Library, and all posted and associated content indicates your acceptance of BioOne's Terms of Use, available at [www.bioone.org/terms-of-use](http://www.bioone.org/terms-of-use).

Usage of BioOne Digital Library content is strictly limited to personal, educational, and non-commercial use. Commercial inquiries or rights and permissions requests should be directed to the individual publisher as copyright holder.

---

BioOne is an innovative nonprofit that sees sustainable scholarly publishing as an inherently collaborative enterprise connecting authors, nonprofit publishers, academic institutions, research libraries, and research funders in the common goal of maximizing access to critical research.

# Remediation of Lead-Contaminated Water Using Green Synthesized Iron-Oxide Nanoparticles: Performance and Mechanism

Air, Soil and Water Research  
Volume 17: 1–11  
© The Author(s) 2024  
Article reuse guidelines:  
sagepub.com/journals-permissions  
DOI: 10.1177/11786221241278517



Linyi Li<sup>1</sup>, Mohammad Aslam Haziq<sup>2</sup>, Sajid Ullah<sup>3,4</sup> ,  
Abdul Ghani Stanikzai<sup>5</sup>, Shah Dehrai Bibi<sup>6</sup>, Taqweem UI Haq<sup>6</sup>,  
Muhammad Tayyeb<sup>7</sup> and Zihua Yang<sup>8</sup>

<sup>1</sup>Shanghai Key Laboratory of New Drug Design, School of Pharmacy, East China University of Science and Technology, Shanghai, China. <sup>2</sup>Department of Water and Environmental Engineering, Kandahar University, Kandahar, Afghanistan. <sup>3</sup>Department of Water Resources and Environmental Engineering, Nangarhar University, Jalalabad, Afghanistan. <sup>4</sup>School of Resources and Environmental Engineering, East China University of Science and Technology, Shanghai, China. <sup>5</sup>Department of Environmental Sciences, International Islamic University Islamabad, Pakistan. <sup>6</sup>State Key Joint Laboratory of Environment Simulation and Pollution Control, School of Environment, Beijing Normal University, Beijing, China. <sup>7</sup>Department of Environmental Sciences, Abdul Wali Khan University, Mardan, Pakistan. <sup>8</sup>School of Chemical Engineering, East China University of Science and Technology, Shanghai, China.

**ABSTRACT:** Lead (Pb(II)) ions in water pose a significant threat to both human health and aquatic ecosystems. Various approaches have been employed for wastewater treatment, but adsorption is often preferred due to its effectiveness. However, its practical application is limited by the large quantities of adsorbent required, which consequently increases operational costs. In this study, orange-modified iron-oxide nanoparticles (O-Fe<sub>3</sub>O<sub>4</sub>) are synthesized from agro-waste mass (orange peel), and adsorption experiments were conducted for the removal of Pb(II) from aqueous solution. Characterization studies confirm that O-Fe<sub>3</sub>O<sub>4</sub> nanoparticles possess a mesoporous hexagonal nanocrystalline structure, with diameters measuring less than 100 nm. The adsorption process was optimized using a central composite design framework combined with response surface methodology. The analysis of interaction effects demonstrated that they significantly influenced the effectiveness of adsorption removal. The study revealed that an initial concentration of 25 mg/L, a dosage of 0.2 g/L, a contact period of 90 min, and a pH of 5.5 were the optimum conditions to achieve above 95% of Pb(II) removal. The green synthesized O-Fe<sub>3</sub>O<sub>4</sub> nanoparticles, which presented high efficacy, makes it a promising option for implementing the sustainable water purification.

**KEYWORDS:** Adsorption method, eco-friendly, lead removal, heavy metals, iron nanoparticles, isotherm study

RECEIVED: April 2, 2024. ACCEPTED: August 12, 2024.

TYPE: Original Research

**CORRESPONDING AUTHOR:** Sajid Ullah, Department of Water Resources and Environmental Engineering, Nangarhar University, Jalalabad, Afghanistan. Email: Sajidjalwan@gmail.com

## Introduction

Lead (Pb(II)) is the second most toxic heavy metal, which comprises 0.002% of Earth's crust it is naturally found in a very limited amount but it is mostly produced due to human-made industries, automobiles, and batteries (Hettiarachchi et al., 2024). Pb(II) accumulates in the water and soil as a result of excessive mining and smelting of Pb-containing metal minerals, burning of fossil fuels, and careless use of Pb(II)-containing chemicals, which has major effects on water and soil lead pollution worldwide (Noman et al., 2022). Recently, the severity of Pb(II)-contaminated water has rapidly increased throughout the world (Ahmed et al., 2023).

In addition, approximately 20 million people living in a high-risk region of Pb(II) contamination (Levin et al., 2021). Pb(II) occurs in different chemical forms in water, soil, and the atmosphere, with varying degrees of bioavailability (Liu et al., 2023). Pb(II) can easily enter the crops through soil or food chain, hence harming the plant, animal, and human health (Raj & Das, 2023). The rapid Pb(II) water contamination and its toxicity around the world attracted the researcher attention to

develop a novel and effective adsorption method for its treatment (Ghani et al., 2022; Hama Aziz et al., 2023). Up to date, different advanced technologies such as phytoremediation, chemical precipitation, electrocoagulation, electro kinetic processes, membrane technology, ion-exchanges, and adsorption method have been applied for the treatment of Pb(II) contaminated water (Hussain et al., 2023; Nawab et al., 2021, 2024; Shaukat et al., 2022; Ullah et al., 2022, 2023; Xie et al., 2022; Yadgari et al., 2023).

In recent years, the adsorption technique has been widely used for Pb(II) contaminated water due to its low-cost, simplicity, porous structure, high surface area, stability, compatibility with soil matrix, high adsorption rate, and more functional groups, thus making it a promising technique and best future alternatives for Pb(II) contaminated water remediation (Awual et al., 2019). Adsorption is a proper Pb(II) treatment method that has been reported to have >99% removal efficiencies for Pb(II) treatment without using chemical addition (Gusain et al., 2019). Specifically, the adsorption method mainly depends on electrostatic forces between molecules that have



Creative Commons Non Commercial CC BY-NC: This article is distributed under the terms of the Creative Commons Attribution-NonCommercial 4.0 License (<https://creativecommons.org/licenses/by-nc/4.0/>) which permits non-commercial use, reproduction and distribution of the work without

been adsorbed and the van der Waals separation process (Gan et al., 2023). However, it is important to note that the effectiveness of adsorption method can be influenced due to temperature, acting pH, exposure time, initial concentration of Pb(II), and adsorbent dose (Nawab et al., 2021, 2023; Tee et al., 2022; Tholley et al., 2023; Z. Yang et al., 2021).

Currently, numerous types of adsorbents have been effectively used for Pb(II) removal comprising activated carbon (Zhang et al., 2021), activated alumina (Ebadollahzadeh & Zabihi, 2020), iron composite (Jin et al., 2023), date palm leaves (Rambabu et al., 2023), agriculture wastes (Ezeonuegbu et al., 2021), granular adsorbents (Xu et al., 2020), iron oxide-coated biochar (Kim et al., 2024), zero valent iron (Tarekegn et al., 2021), iron oxides-coated sand (Boujelben et al., 2010), waste-based nano-activated carbon (Rambabu, AlYammahi, et al., 2021), and chitosan (Lu et al., 2013).

In current research, a series of orange-modified iron-oxide nanoparticles (O-Fe<sub>3</sub>O<sub>4</sub>) with various pH values were synthesized. The chemical composition of synthesized O-Fe<sub>3</sub>O<sub>4</sub> were studied through FTIR, XRD, BET, SEM, and XPS methods. The use of O-Fe<sub>3</sub>O<sub>4</sub> nanoparticles is eco-friendly due to its natural abundance and biodegradability, minimizing the need for toxic chemicals and energy-intensive processes. Furthermore, the extract bioactive compounds serve as effective reducing and stabilizing agents, contributing to sustainable nanoparticles production with minimum environmental impacts. This approach aligns with green chemistry principles, promoting a more environmentally conscious method for nanoparticles synthesis. The O-Fe<sub>3</sub>O<sub>4</sub> nanoparticles with maximum Pb(II) adsorption capability were reported. The present study shown the capability of O-Fe<sub>3</sub>O<sub>4</sub> to efficiently adsorb Pb(II) from wastewater and thus providing theoretical base for agro-waste applications toward water treatment.

## Materials and Methods

### Chemicals and reagents

Reagents used in current study namely, Lead Nitrate (Pb(NO<sub>3</sub>)<sub>2</sub>), Sodium Hydroxide (NaOH), Iron powder, Potassium Permanganate (KMnO<sub>4</sub>), Hydrochloric acid (HCl), and Ethanol were of analytical grade and purchased from Shanghai Macklin Biochemical Co., Ltd. Orange peels were collected from the local market of Shanghai, China. About 0.1 M NaOH and 0.1 M HCl were used for the adjustment of pH. Whatman 42 filter paper was used for separating the adsorbent from water. The desired amount of (Pb(NO<sub>3</sub>)<sub>2</sub>) was dissolved in deionized water to get 1000 mg/L stock solution that was used for further experiments.

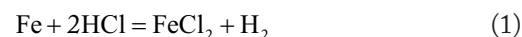
### Preparation of stock solution of Pb(II)

About 1000 mg/L of Pb(II) stock solution was prepared by dissolving 1.614 g of (Pb(NO<sub>3</sub>)<sub>2</sub>) in 11 of distilled water. The

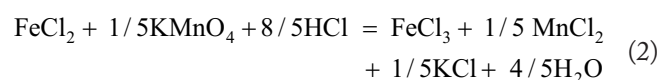
50 mg/L standard Pb solution was prepared from 1000 mg/L Pb(II) solution by serial dilution method.

### Synthesis of FeCl<sub>2</sub> and FeCl<sub>3</sub>

A total five (05) g of iron powder was dissolved in 150 mL of 2M HCl solutions to make 150 mL of FeCl<sub>2</sub>. The chemical reaction is shown in equation (1).



A 1 M of FeCl<sub>3</sub> is obtained by adding 1.5 g of KMnO<sub>4</sub> in 78.0 mL of 35% HCl and 50 mL of FeCl<sub>2</sub>. Color was changed from green to brown after the formation of FeCl<sub>3</sub>. Both solutions were filtered with Whatman filter paper. Chemical reaction is shown in equation (2).

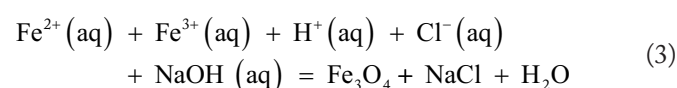


### Synthesis of orange peel extract

The orange peel was collected from local market located at Shanghai, China. The collected peel was initially washed with tap water followed by deionized water several times to make it dust free. Further, the peel was dried at room temperature for 20 days in dust free environment. Then, the dried peel was crushed using pestle and mortar and sieved through 0.5 mm size of sieve. About 25 g powder was added to 250 mL of distilled water and sonicated by using probe sonicator for 20 min. After that the obtained mixture was filtered using Whatman filter 42 and centrifuged at 4000 rpm for 30 min to remove the powder particles. The obtained supernatant which acts as capping agent and reducing agent was cooled at room temperature and stored in a refrigerator at 5°C temperature for future use.

### Synthesis of iron oxide nanoparticles (Fe<sub>3</sub>O<sub>4</sub>)

Fe<sub>3</sub>O<sub>4</sub> nanoparticles have been synthesized by co-precipitation method. FeCl<sub>3</sub> and FeCl<sub>2</sub> were mixed in 2:1 ratio at open atmosphere. It may be possible that some portion of FeCl<sub>2</sub> got converted into FeCl<sub>3</sub>. To counteract the converted portion of FeCl<sub>3</sub> and FeCl<sub>2</sub> were mixed with 100 mL of orange peel extract in 2:1 ratio. Color was changed immediately from yellow to black after the addition of peel extract. The obtained solution was then heated at 80°C temperature using heating mantle. About 1 M freshly prepared NaOH was added drop wise to the solution under continuous stirring mode until the pH of the solution raised to pH 10. The solution mixture was stirred for 45 min to maintain the homogeneity of the solution during the reaction process. The overall reaction is given in equation 3.



The prepared  $\text{Fe}_3\text{O}_4$  nanoparticles was collected by using centrifuge technique. Later, the nanoparticles were washed several times using deionized water and ethanol to remove the impurities. The precipitate was kept for drying in vacuum oven for 3 to 4 days at  $60^\circ\text{C}$  temperature for future use.

### Instruments for adsorbent characterization

The analytical techniques, including Fourier Transform Infrared Spectroscopy (FT-IR; PerkinElmer, USA), X-ray diffractometer (XRD; Hitachi, Japan), X-ray photoelectron spectroscopy (XPS; PerkinElmer, USA), Scanning electron microscopy (SEM; Hitachi, Japan), Scanning electron microscopy with energy dispersive X-ray spectroscopy (SEM/EDX; PerkinElmer, USA) were used to assess the chemical structure and physical texture of synthesized O- $\text{Fe}_3\text{O}_4$  nanoparticles, respectively. High-resolution Transmission Electron Microscope (HR-TEM; JEOL, USA) was used to measure the particle size and shape of O- $\text{Fe}_3\text{O}_4$  nanoparticles. Field-emission scanning electron microscopy (FE-SEM; JEOL, USA) was used for mapping. The amount of Pb(II) ion was measured using the Inductive coupled plasma-optical emission spectroscopy (ICP-OES; PerkinElmer, USA).

### Theory

To find out the effect of various operating conditions on the adsorption process batch adsorption study was conducted. To optimize the maximum removal efficiency of Pb(II), the batch experiments were carried out by varying the dose, time, pH, and initial concentration of the aqueous solution. The removal efficiency of Pb(II) was calculated as per the following equation (4) described by Rambabu et al. (2019) and Rambabu, Thanigaivelan, et al. (2021).

$$\text{Removal efficiency, } R = ((C_0 - C_e) / C_0) * 100\% \quad (4)$$

Where,  $C_0$  = initial concentration of Pb(II) in synthetic Pb(II) solution in mg/L,  $C_e$  = Residual concentration of Pb(II) after equilibrium in mg/L.

The Adsorption capacity of adsorbent was calculated as per the following equation (5).

$$q \text{ (mg / gm)} = ((C_0 - C_e) * V) / 1000m \quad (5)$$

Where,  $m$  = mass of the adsorbent in g and  $V$  = volume of solution in mL.

### Experimental design

To examine the efficiency of Pb(II) adsorption using O- $\text{Fe}_3\text{O}_4$  nanoparticles and to determine the interaction between the independent process variables on the removal efficiency, different experiments were conducted in a holistic way. In current research, it was reported that the Pb(II) removal efficacy was

found to be highly dependent on initial concentration, pH, adsorbent dosage, and contact time. Each variable may affect the removal efficiency differently depending on how much of an impact it has. As there will be variations in the permutations and combinations to do experiments for varying ranges of every variable. Designing the experiment matrix in a way that minimizes the number of experiments and, consequently, lowers chemical waste is therefore necessary. In order to do this, a methodical approach is taken, and as Table 1 shows, an experimental matrix is created utilizing the face central composite design (FCCD). The range of each process variable is systematically chosen, based on the stronger influence on the adsorption efficiency. Using the strongest influence on the adsorption efficiency as a guide, the range of each process variable is rigorously selected. As Table 1 illustrates, 30 sets of experimental runs representing various space types in a cubic representation are carried out.

## Results and Discussion

### Characterization of adsorbent

The shape and elemental characteristics of the synthesized nanoparticles were examined by SEM, SEM-EDX, and FE-SEM mapping. A hexagonal form with a diameter of less than 100 nm and mesoporous crystalline structure is visible in the SEM image of the manufactured O- $\text{Fe}_3\text{O}_4$  nanoparticles as shown in Figure 1a. Many active sites for the adsorption of Pb(II) were produced by this porous surface. Additional SEM-EDX micrographs as given in Figure 1b of the O- $\text{Fe}_3\text{O}_4$  nanoparticles show the presence of iron oxide nanoparticles along C and O, which signifies the capping of iron oxide on orange peel extract. Iron oxides are present along with O and C, as demonstrated by the FE-SEM elemental mapping of O- $\text{Fe}_3\text{O}_4$  nanoparticles in Figure 1c.

HR-TEM images (Figure 1d–g) further validated the size and hexagonal crystalline structure of O- $\text{Fe}_3\text{O}_4$  nanoparticles. The TEM analysis clearly confirms that the O- $\text{Fe}_3\text{O}_4$  nanoparticles have a hexagonal crystalline form with an average particle size of approximately 55 nm. The absence of substantial  $\text{Fe}_3\text{O}_4$  nanoparticles aggregation was observed as shown in Figure 1e–f. The structure and texture of the synthesized adsorbent were examined using X-ray diffraction (XRD) as given in Figure 2a. The results obtained in this study align with findings reported by other researchers (Basavegowda et al., 2014). XPS analysis were carried out to determine the elemental or chemical composition of the synthesized O- $\text{Fe}_3\text{O}_4$  nanoparticles as shown in Figure 2b. The presence of C, O, and  $\text{Fe}_3\text{O}_4$  was clearly observed as given in Figure 2b.

The  $\text{Fe}2p_{1/2}$  and  $\text{Fe}2p_{3/2}$  peaks from  $\text{Fe}_3\text{O}_4$  are indicated by the strong peaks between 710 and 730 eV, together with C1s at 282 eV and O1s at 528 eV. These findings validate the synthesis of O- $\text{Fe}_3\text{O}_4$  nanoparticles. Furthermore, the FT-IR was used to examine the functional groups on the surface and vibrational characteristics of the O- $\text{Fe}_3\text{O}_4$  nanoparticles. The

**Table 1.** Design of Experimental Matrix Considered for Pb(II) Adsorption.

RUN	INITIAL CONCENTRATION (G/L)	DOSAGE (MG/L)	CONTACT TIME (MIN)	PH	PB(II) REMOVAL (%)	SPACE TYPE
1	30	0.35	90	5.5	95.12	Factorial
2	30	0.40	55	7.5	69.25	Factorial
3	60	0.55	80	5.5	61.63	Center
4	60	0.55	100	5.5	59.78	Axial
5	60	0.75	90	5.5	75.66	Axial
6	60	0.40	90	5.5	59.98	Axial
7	60	0.55	90	6.5	49.95	Axial
8	60	0.15	90	6.5	43.76	Axial
9	80	0.30	75	5.5	40.16	Factorial
10	80	0.30	50	5.5	30.88	Factorial
11	80	0.50	50	4.5	39.65	Factorial
12	80	0.25	50	4.5	30.10	Factorial
13	60	0.55	80	3.5	60.83	Center
14	60	0.55	80	3.5	61.15	Center
15	40	0.25	75	5.0	58.87	Factorial
16	45	0.50	75	5.0	60.20	Factorial
17	75	0.55	60	6.5	40.80	Axial
18	65	0.65	50	6.0	50.80	Factorial
19	45	0.50	65	7.5	64.79	Center
20	35	0.60	85	5.0	78.98	Factorial
21	55	0.45	80	4.5	60.34	Center
22	35	0.30	55	5.0	55.67	Factorial
23	35	0.60	55	5.0	70.10	Factorial
24	35	0.60	75	5.0	80.55	Factorial
25	50	0.35	60	6.0	65.25	Center
26	55	0.75	70	5.0	55.65	Factorial
27	55	0.75	90	5.5	38.78	Factorial
28	20	0.50	85	7.0	86.14	Axial
29	40	0.55	30	4.0	29.33	Axial
30	30	0.20	30	5.0	60.58	Factorial

mesoporous hexagonal nano-crystalline structure of the O-Fe<sub>3</sub>O<sub>4</sub> nanoparticles is confirmed by the whole characterization tests. Additionally, UV-Visible spectroscopy was used to prove the stability and generation of the green synthesized O-Fe<sub>3</sub>O<sub>4</sub> nanoparticles in aqueous solution as shown in Figure 2c. UV-spectrum indicating the high purity of the synthesized O-Fe<sub>3</sub>O<sub>4</sub> nanoparticles using this technique.

#### *Effect of adsorbent dose variation*

The impacts of available active sites on the adsorption process were investigated by a dose variation test. The experimental results demonstrated the adsorbent strong adsorption capacity, with more than 95% removal efficiency at 0.20g/L of adsorbent dose as reported in Figure 3. More active sites that are

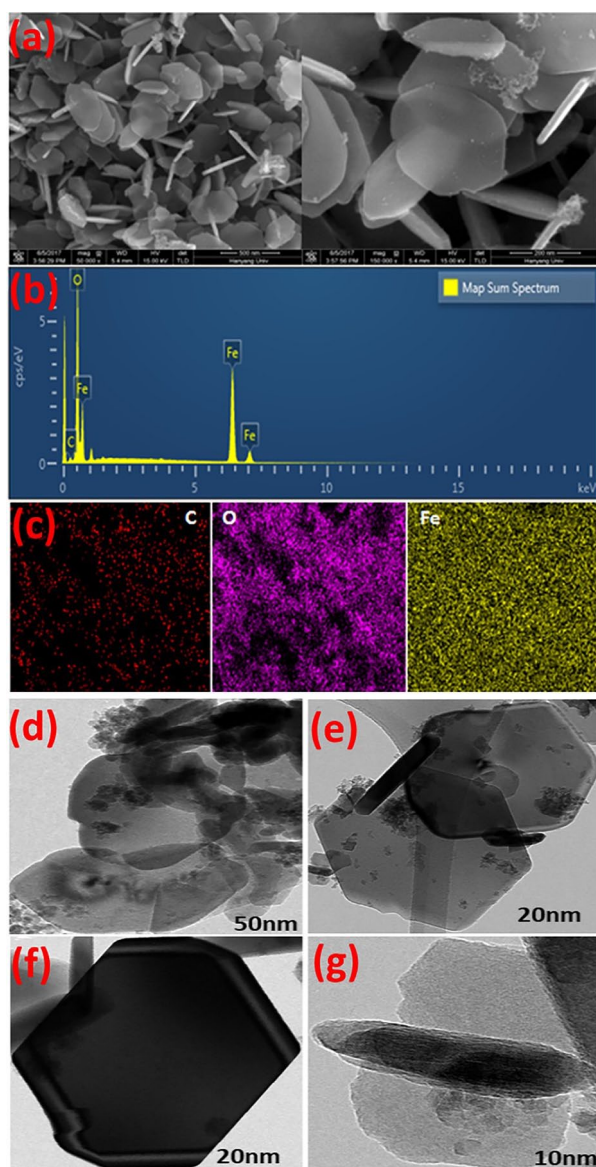


**Figure 1.** (a) SEM image, (b) SEM-EDX elemental analysis, (c) FE-SEM elemental mapping images, and (d–g) HR-TEM images of O-Fe<sub>3</sub>O<sub>4</sub> nanoparticles.

available for sorption on the surface of O-Fe<sub>3</sub>O<sub>4</sub> nanoparticles often result in an increase in Pb(II) adsorption. At 2.0 g/L of adsorbent, the removal rate achieved 99%. The study concluded that by adding a small dose of O-Fe<sub>3</sub>O<sub>4</sub> nanoparticles to the aqueous solution, a higher removal efficiency of Pb(II) ions can be achieved. This enhanced efficiency is due to the O-Fe<sub>3</sub>O<sub>4</sub> nanoparticles high affinity for Pb(II) ions, which allows them to effectively adsorb and remove the Pb(II) from the solution even at low concentrations. Noman et al. (2022) reported that the Pb(II) adsorption was effective at NPs:Pb(II) ratios of 1:5 and 1:10 with the removal efficacy of 90% and 78%, respectively. Tabesh et al. (2018) also tested three different doses of nano-sized  $\gamma$ -Al<sub>2</sub>O<sub>3</sub> nanoparticles such as (100, 50, and 10 mg/L) for Pb(II) adsorption. The results proved that when the nanoparticles were added up to 100 mg/L, the Pb(II) adsorption improved.

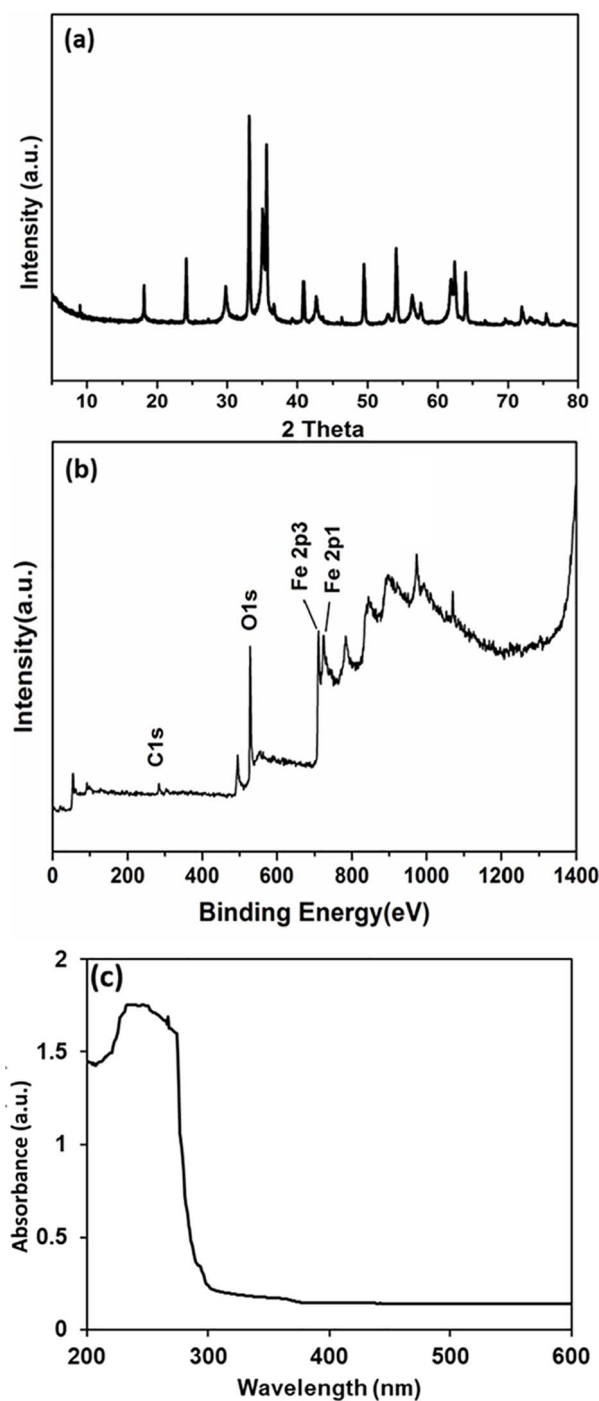


**Figure 2.** (a) XRD, (b) displays the nanoparticles XPS spectra, and (c) UV-Visible spectrum of O-Fe<sub>3</sub>O<sub>4</sub> nanoparticles.

#### *Effect of contact time and initial concentration*

To determine the optimum adsorption time for Pb(II) ions, an experiment was conducted using O-Fe<sub>3</sub>O<sub>4</sub> nanoparticles in an aqueous solution. The experimental conditions were maintained with a constant adsorbent dose of 0.2 g/L and a Pb(II) concentration of 30 mg/L. As illustrated in Figure 4, the removal efficiency of Pb(II) ions increased with longer contact times. The results indicated that equilibrium was reached at 90 min for Pb(II) ions. Approximately 85% of the Pb(II) was removed

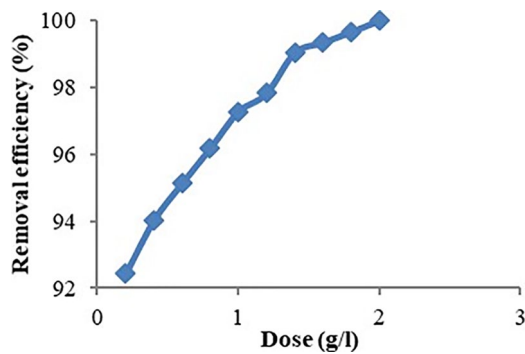


**Figure 3.** Effect of dose variation on Pb(II) adsorption using O-Fe<sub>3</sub>O<sub>4</sub> nanoparticles.

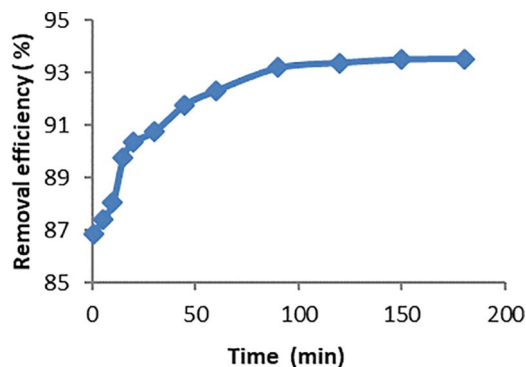


**Figure 4.** Effect of contact time on Pb(II) adsorption using O-Fe<sub>3</sub>O<sub>4</sub> nanoparticles.

within the 10 min of contact time, and almost above 90% was removed after an additional 30 min. These findings suggest that a significant portion of Pb(II) ion removal occurs rapidly within the initial stages of the adsorption process. The reason for this could be attributed to the O-Fe<sub>3</sub>O<sub>4</sub> nanoparticles small size, which facilitated the diffusion of Pb(II) ions from bulk solution onto the solid surface-active sites. Regarding the adsorption of other metal ions onto iron oxide nanoparticles, the short equilibrium period is consistent with that reported by previous researchers (Sun et al., 2007; Uheida et al., 2006). Additionally, according to Pal et al. (2018) the sulfide adsorption on Alg/iron oxide-NP beads reached equilibrium in less than 3 h.

The purpose of the initial concentration research was to investigate how the strength of the adsorbate affected the process of adsorption. As seen in Figure 5, a very high removal efficiency (>95%) was achieved up to an initial concentration of 25 mg/L at a constant adsorbent dose of 0.2 g/L in the solution. The removal efficiency then rapidly reduced to 91% when the initial concentration increased to 40 mg/L. Up to a certain level, adsorption increases because the adsorbent's available surface, or active sites, are large enough to adsorb the majority of Pb(II) ions at low initially concentrations. The removal effectiveness decreases with further increases in the initial concentration because there are no longer enough sites available to absorb Pb(II). It obviously means that there is enough adsorption capacity of the adsorbent to remove Pb(II) from water

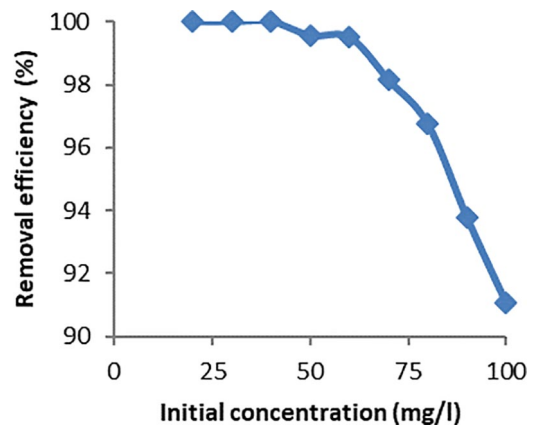


**Figure 5.** Effect of initial concentration of O-Fe<sub>3</sub>O<sub>4</sub> nanoparticles on Pb(II) adsorption.

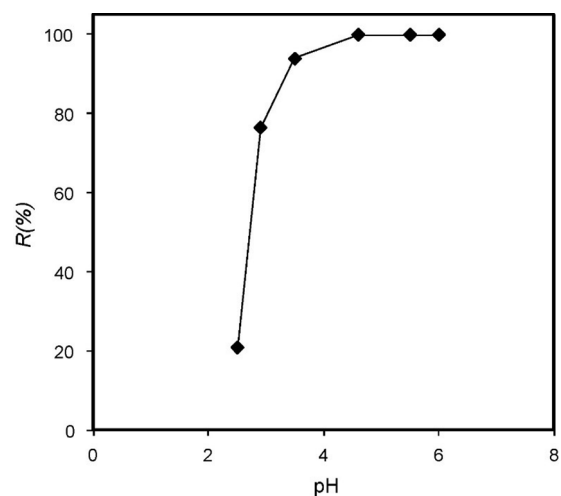


**Figure 6.** Effect of pH on Pb(II) adsorption onto O-Fe<sub>3</sub>O<sub>4</sub> nanoparticles.

solutions. Noman et al. (2022) reported that the adsorption of Pb(II) was efficient and approximately 90% of Pb(II) removed with the initial concentration of adsorbent. The adsorption of Pb(II) with adsorbents was observed with the initial concentrations of 95 and 162 mg/L, respectively. Results showed that the Pb(II) was adsorbed on the surface of adsorbents quickly, and equilibrium was attained within 30 min (Nassar, 2010).

#### *Effect of pH on Pb(II) adsorption*

The adsorption process is known to be significantly impacted by pH. The impact of pH on the adsorption process was examined at various pH intervals in the solution because variations in pH have a major impact on the chemistry of the metal ions solution and the surface. The investigation was carried out with a fixed concentration of Pb(II) 30 mg/L and adsorbent dose 0.2 g/L. For Pb (II) solution, the pH value was ranged between 2 and 12. The result presented in Figure 6 indicates a significant rise in the percentage of Pb(II) adsorption by O-Fe<sub>3</sub>O<sub>4</sub> nanoparticles, from 10% to 95% at pH 2 to pH 5.5, respectively. Because of the presence of significant positive charge H<sup>+</sup>

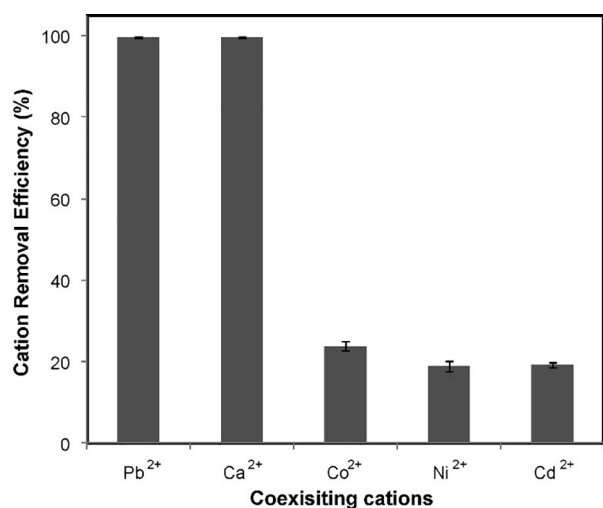


**Figure 7.** Effect of coexisting ions on Pb(II) adsorption using O-Fe<sub>3</sub>O<sub>4</sub> nanoparticles.

ions surrounding the surface of the adsorbent and free Pb(II) ions in the solution at lower pH values, electrostatic repulsion cannot remove the Pb(II) ions from the solution (Wang et al., 2013). As the pH rises, electrostatic repulsion begins to decrease, which results in an increase in removal efficiency of Pb(II) ions (Nassar, 2010).

The adsorption efficacy is highly increased at pH 5.5 due to no electrostatic repulsion. It is evident that Pb(II) ion removal is pH dependent, with pH 5.5 showing the maximum adsorption. Such pH effect was reported for the Pb(II) adsorption using bulk iron oxides (Lee et al., 1998). Increased pH promotes the deprotonation of sorbent surfaces (Prasad et al., 2022). The adsorption capacity increases as a result of increased deprotonation because it increases the negatively charged sites. These sites strengthen the attractive interactions between the sorbent surface and the Pb(II) ions. However, in the lower pH range, the predominance of positively charged sites increases the repulsion forces between the Pb(II) ions and the sorbent surface, which reduces the adsorption of Pb(II) ions (Xiong et al., 2021).

#### *Effect of coexisting cations*

Wastewater typically contain many cations. Therefore, the effectiveness of Pb(II) removal may be affected by the presence of other cations. Thus, the influence of Ca<sup>2+</sup>, Ni<sup>2+</sup>, Co<sup>2+</sup>, and Cd<sup>2+</sup> coexisting cations on Pb(II) adsorption were investigated. The means of four duplicate runs with newly prepared samples conducted on various days are given in Figure 7. Remarkably, the removal effectiveness of Pb(II) is not significantly affected by the presence of these coexisting cations. However, Ca<sup>2+</sup> ions and some of the Co<sup>2+</sup>, Ni<sup>2+</sup>, and Cd<sup>2+</sup> ions were adsorbed on the surface of O-Fe<sub>3</sub>O<sub>4</sub> nanoparticles. The competitive adsorption ability of metal ions is often dependent on several parameters, including the metal's hydration energy, molecular mass, ion charges, and hydrated ionic

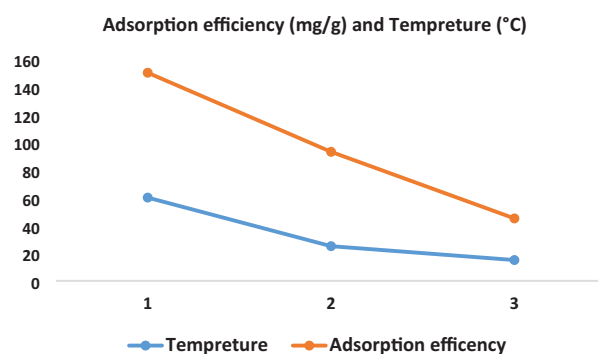


**Figure 8.** Effect of temperature on the adsorption of Pb(II) using O-Fe<sub>3</sub>O<sub>4</sub> nanoparticles.

radius (Lv et al., 2005). A multi-surface adsorption is suggested by the fact that the coexisting cations did not appear to compete with Pb(II) ions for the active sites on the O-Fe<sub>3</sub>O<sub>4</sub> nanoparticles (Benjamin & Leckie, 1981).

#### *Effect of temperature*

The adsorption process is significantly influenced by temperature (Rodda et al., 1996). To explore the effects of temperature on Pb(II) adsorption capability, temperature-dependent experiments were conducted. At various temperatures, the Pb(II) adsorption isotherms onto O-Fe<sub>3</sub>O<sub>4</sub> were investigated, as indicated in Figure 8. The quantity of Pb(II) adsorbed per unit area of the adsorbent improved with increasing temperature. This implies the endothermic and spontaneous nature of the adsorption process. Pb(II) adsorption ability was examined in this study at three different temperatures, as shown in Figure 8. On the other hand, the influence of temperature on Pb(II) adsorption relates to how temperature variations might affect lead ion adsorption onto a certain material or adsorbent process.

This is usually investigated to learn how temperature impacts the thermodynamics of the adsorption reaction as well as the adsorption capacity (S. Yang et al., 2010) carried out a similar investigation and found that temperature is important for the adsorption of Pb(II) from water systems. They also verified that the adsorption process is endothermic and spontaneous. Zhang et al. (2021) and Z.-H. Huang et al. (2011) likewise came to the conclusion that an endothermic process was occurring in their investigation and Pb(II) adsorption efficiency improved as temperatures increased. Nassar (2010) conducted a series of experiments at 298, 313, and 328 K to study the influence of temperature on Pb(II) adsorption. Results showed that the amount of Pb(II) adsorbed onto Fe<sub>3</sub>O<sub>4</sub> nanoparticles increases as the temperature increased. Pb(II) adsorption may increase with temperature because of increased ion mobility, which raises the quantity of ions interacting with active sites at adsorbent surfaces. Other researchers have observed similar findings regarding Pb(II) adsorption on oxide-based surface (Eren, 2009; Y.-H. Huang et al., 2007).

**Table 2.** Kinetics Parameters for the Adsorption of Pb(II) Using O-Fe<sub>3</sub>O<sub>4</sub> Nanoparticles (0.2g/L) at pH 5.5.

PB(II) CONCENTRATION (PPM)	QE, TH, MG/G	PSEUDO-FIRST ORDER (PFO)			PSEUDO-SECOND ORDER (PSO)		
		QE, CAL, MG/G	$K_1$	$R^2$	QE, CAL, MG/G	$K_2$	$R^2$
10	17.12	2.86	0.16	.066	16.10	0.006	.996
20	31.64	21.08	0.03	.014	31.97	0.003	.999

**Table 3.** Adsorption Isotherm Parameters of Pb(II) using O-Fe<sub>3</sub>O<sub>4</sub> Nanoparticles (0.2g/L) at pH of 5.5 and 90 min.

TEMPERATURE (°C)	LANGMUIR			FREUNDLICH		
	$Q_{MAX}$ (MG/G)	$K_L$ (L/MG)	$R^2$	$K_F$ , MG/G (L/MG) <sup>1/N</sup>	$N$	$R^2$
15	30.87	0.33	.996	21.42	2.26	.952
25	68.00	0.29	.997	16.76	2.40	.966
60	90.10	0.24	.999	7.75	1.50	.985

### Adsorption mechanism

The adsorption mechanism of Pb(II) ions on O-Fe<sub>3</sub>O<sub>4</sub> nanoparticles, which are iron oxide nanoparticles coated with orange peel extract, involves a combination of physical and chemical processes. The high surface area and magnetic properties of O-Fe<sub>3</sub>O<sub>4</sub> nanoparticles provide numerous active sites for the adsorption of Pb(II) ions (Zannotti et al., 2024). The orange peel extract coating introduces additional functional groups, such as hydroxyl (-OH) and carboxyl (-COOH) groups, which enhance the chemical affinity between the nanoparticles and the Pb(II) ions (Zannotti et al., 2024). These functional groups facilitate chemisorption through the formation of strong chemical bonds with Pb(II) ions, resulting in stable adsorption complexes (Xiao et al., 2020). Additionally, the negatively charged surface of O-Fe<sub>3</sub>O<sub>4</sub> nanoparticles at certain pH levels promotes electrostatic interactions with the positively charged Pb(II) ions, further increasing the adsorption capacity (He et al., 2016). The combined effects of surface adsorption, electrostatic attraction, and chemisorption contribute to the high efficiency and rapid removal of metal ions from aqueous solutions (Erattamparambil et al., 2023). This multifaceted adsorption mechanism underscores the potential of O-Fe<sub>3</sub>O<sub>4</sub> nanoparticles as a highly effective and eco-friendly material for the remediation of Pb(II)-contaminated water.

Electrostatic attraction is most likely the mode of adsorption (Liang et al., 2017). The negatively charged surface of the adsorbent and the Pb(II) exhibit a notably strong electrostatic interaction in the basic solution. The number of positively charged and negatively charged sites rises and falls in proportion to the solution decreasing pH (Oladoye, 2022). The adsorption of Pb(II) ions is not favored by a positively charged surface site on the nanoparticles because of electrostatic repulsion. Furthermore, in an acidic environment with low pH levels, surplus hydrogen ions compete with Pb(II) ions for the adsorption site, which reduces Pb(II) adsorption.

### Kinetic model

Pseudo-first order (PFO) and pseudo-second order (PSO) models were used to examine the experimental equilibrium kinetic data in order to understand the kinetics of this adsorption process. The parameters of these two kinetic models are displayed in Table 2. The results indicate that the PSO kinetic model explained the adsorption kinetics more clearly than the PFO kinetic model. The results also imply that Pb(II) adsorption kinetics are governed by rate-diffusion-controlled surface kinetics. For the pseudo-second order reaction model and pseudo first order reaction model, respectively, the measured correlation coefficients ( $R^2$ ) values are .996 and .999, respectively.

### Isotherm model

To investigate the process of adsorption mechanism, various isotherm models were employed in conjunction with the isotherm data. To examine Pb(II) adsorption behavior, experimental data were applied to the Freundlich and Langmuir isotherm models. The results are showed in Table 3. To determine the Freundlich isotherm,  $K_F$  and  $n$  are the isotherm parameters. In adsorption research, the Freundlich and Langmuir isotherms are often utilized models. The Freundlich model is more adaptable and may describe multilayer adsorption on heterogeneous surfaces, whereas the Langmuir model presupposes a monolayer adsorption mechanism on a homogeneous surface.

The results as given in Table 3 following the examination and fitting of the experimental data to both models. The Langmuir model was found to offer the greatest fit to the adsorption equilibrium data based on the data presented in Table 3. This indicates that a monolayer adsorption process on a homogeneous and uniform surface is the most accurate way to characterize the adsorption of Pb(II) onto O-Fe<sub>3</sub>O<sub>4</sub> nanoparticles. This finding suggests that Pb(II) adsorption onto

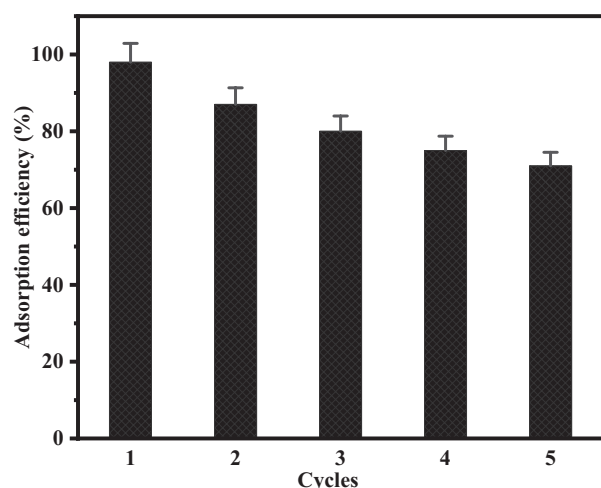


**Figure 9.** Reusability of O-Fe<sub>3</sub>O<sub>4</sub> nanoparticles for adsorption/desorption of Pb(II) during five cycles.

O-Fe<sub>3</sub>O<sub>4</sub> nanoparticles is a one-layer thick process in practice, with Pb(II) ions attaching to accessible binding sites on the surface in a manner consistent with the Langmuir model's presumptions. Using O-Fe<sub>3</sub>O<sub>4</sub> nanoparticles as an adsorbent, these insights can be useful in the design and optimization of adsorption procedures for the removal of Pb(II).

#### Reusability of adsorbents

A 10-mL solution with an initial Pb(II) concentration of 150 mg/L at pH 5.5 is used to calculate the removal efficiency, or R(%), of Pb(II) over the course of five cycles of adsorption, desorption, and regeneration as shown in Figure 9. As can be observed, throughout the course of the five cycles, there was no significant decrease in the adsorption capacity of O-Fe<sub>3</sub>O<sub>4</sub> nanoparticles. The outcomes showed that O-Fe<sub>3</sub>O<sub>4</sub> nanoparticles are suitable for the design of a continuous process since they may be utilized to remove and recover metal ions from wastewater across a number of cycles. Regeneration is necessary for commercially accessible adsorbents such as activated carbons, which are expensive and time-consuming.

In reality, the expensive aspect of the adsorption method is the regeneration and recovery of spent activated carbons, making up to 75% of the overall expenses associated with operation and maintenance (Jaria et al., 2022). Hence, O-Fe<sub>3</sub>O<sub>4</sub> nanoparticles cost-effective alternative with a fast rate of adsorption; additionally, it can be easily regenerated and may not even be required for in situ use.

#### Limitations and future prospects

The current study successfully proved the effectiveness of green-synthesized O-Fe<sub>3</sub>O<sub>4</sub> nanoparticles derived from orange peel extract in removing Pb(II) ions from contaminated water, however, several limitations should be acknowledged. Firstly, the study primarily focused on laboratory-scale experiments, which may not fully represent real-world conditions and

challenges encountered in large-scale water treatment facilities. Secondly, the long-term stability and potential release of nanoparticles into the environment were not extensively investigated. Additionally, the specific interactions and fate of nanoparticles in complex aqueous matrices and diverse environmental settings warrant further exploration. Addressing these limitations through future research will enhance the applicability and reliability of O-Fe<sub>3</sub>O<sub>4</sub> nanoparticles for sustainable remediation of Pb(II) contaminated water.

#### Conclusions

The results of this work revealed that O-Fe<sub>3</sub>O<sub>4</sub> nanoparticles could be a viable replacement for traditional adsorbents in the rapid and highly efficient removal of heavy metal ions such as Pb(II) from wastewater. Adsorption on the surface of O-Fe<sub>3</sub>O<sub>4</sub> nanoparticles proved to be an effective method for removing Pb(II), a common metal ion found in wastewater. Equilibrium was reached in less than 30 min due to the highly rapid adsorption. Additionally, initial Pb(II) concentration, pH, and temperature all had a significant impact on adsorption. At pH 5.5, the greatest removal was noted. Adsorption further increased as temperature and Pb(II) initially concentration increased. Additionally, the adsorption isotherms have been determined and found to be well-fitting to the Freundlich model as compared to the Langmuir model, with both models providing suitable descriptions.

The adsorption of Pb(II) onto O-Fe<sub>3</sub>O<sub>4</sub> nanoparticles was found to be spontaneous, endothermic, and physisorbed due to the thermodynamics of the process. Studies on regeneration and desorption showed that nanoparticles can be used continuously without affecting their ability to adsorb substances. As a result, O-Fe<sub>3</sub>O<sub>4</sub> nanoparticles are suggested as simple and cost-effective adsorbents for the efficient removal and recovery of metal ions from wastewater discharges.

#### Acknowledgements

We would like to express our heartfelt appreciation to all funding sources and anonymous reviewers.

#### Author Contributions

Linyi Li and Sajid Ullah: Data curation, Methodology, Writing—original draft, and Writing—review & editing. Mohammad Aslam Haziq and Abdul Ghani Stanikzai: Draft revising and Writing—review & editing. Shah Dehrai Bibi, Taqweem Ul Haq, Muhammad Tayyab, and Zihua Wang: Writing—review & editing and Resources.

#### Declaration of Conflicting Interests

The author(s) declared no potential conflicts of interest with respect to the research, authorship, and/or publication of this article.

#### Funding

The author(s) received no financial support for the research, authorship, and/or publication of this article.

## ORCID iD

Sajid Ullah  <https://orcid.org/0000-0002-5079-3761>

## REFERENCES

- Ahmed, W., Mehmood, S., Mahmood, M., Ali, S., Shakoor, A., Núñez-Delgado, A., Asghar, R. M. A., Zhao, H., Liu, W., & Li, W. (2023). Adsorption of Pb(II) from wastewater using a red mud modified rice-straw biochar: Influencing factors and reusability. *Environmental Pollution*, 326, Article 121405. <https://doi.org/10.1016/j.envpol.2023.121405>
- Awual, M. R., Hasan, M. M., Islam, A., Rahman, M. M., Asiri, A. M., Khaleque, Md. A., & Sheikh, M. C. (2019). Offering an innovative composited material for effective lead(II) monitoring and removal from polluted water. *Journal of Cleaner Production*, 231, 214–223. <https://doi.org/10.1016/j.jclepro.2019.05.125>
- Basavegowda, N., Somai Magar, K. B., Mishra, K., & Lee, Y. R. (2014). Green fabrication of ferromagnetic Fe<sub>3</sub>O<sub>4</sub> nanoparticles and their novel catalytic applications for the synthesis of biologically interesting benzoxazinone and benzothioxazinone derivatives. *New Journal of Chemistry*, 38(11), 5415–5420. <https://doi.org/10.1039/C4NJ01155D>
- Benjamin, M. M., & Leckie, J. O. (1981). Multiple-site adsorption of Cd, Cu, Zn, and Pb on amorphous iron oxyhydroxide. *Journal of Colloid and Interface Science*, 79(1), 209–221. [https://doi.org/10.1016/0021-9797\(81\)90063-1](https://doi.org/10.1016/0021-9797(81)90063-1)
- Boujelben, N., Bouzid, J., Elouear, Z., & Feki, M. (2010). Retention of nickel from aqueous solutions using iron oxide and manganese oxide coated sand: Kinetic and thermodynamic studies. *Environmental Technology*, 31(14), 1623–1634. <https://doi.org/10.1080/09593330.2010.482148>
- Ebadollahzadeh, H., & Zabihi, M. (2020). Competitive adsorption of methylene blue and Pb (II) ions on the nano-magnetic activated carbon and alumina. *Materials Chemistry and Physics*, 248, Article 122893. <https://doi.org/10.1016/j.matchemphys.2020.122893>
- Erattemparambil, K., Mohan, L., Gnanasundaram, N., & Krishnamoorthy, R. (2023). Insights into adsorption theory of phenol removal using a circulating fluidized bed system. *Arabian Journal of Chemistry*, 16(6), Article 104750. <https://doi.org/10.1016/j.arabjc.2023.104750>
- Eren, E. (2009). Removal of lead ions by Unye (Turkey) bentonite in iron and magnesium oxide-coated forms. *Journal of Hazardous Materials*, 165(1–3), 63–70. <https://doi.org/10.1016/j.jhazmat.2008.09.066>
- Ezeonuegbu, B. A., Machido, D. A., Whong, C. M. Z., Japhet, W. S., Alexiou, A., Elazab, S. T., Qusty, N., Yaro, C. A., & Batiha, G. E.-S. (2021). Agricultural waste of sugarcane bagasse as efficient adsorbent for lead and nickel removal from untreated wastewater: Biosorption, equilibrium isotherms, kinetics and desorption studies. *Biotechnology Reports*, 30, Article e00614. <https://doi.org/10.1016/j.btre.2021.e00614>
- Gan, G., Fan, S., Li, X., Zhang, Z., & Hao, Z. (2023). Adsorption and membrane separation for removal and recovery of volatile organic compounds. *Journal of Environmental Sciences*, 123, 96–115. <https://doi.org/10.1016/j.jes.2022.02.006>
- Ghani, J., Nawab, J., Faiq, M. E., Ullah, S., Alam, A., Ahmad, I., Ali, S. W., Khan, S., Ahmad, I., Muhammad, A., Ur Rahman, S. A., Abbas, M., Rashid, A., Hasan, S. Z., & Hamza, A. (2022). Multi-geostatistical analyses of the spatial distribution and source apportionment of potentially toxic elements in urban children's park soils in Pakistan: A risk assessment study. *Environmental Pollution*, 311, Article 119961. <https://doi.org/10.1016/j.envpol.2022.119961>
- Gusain, R., Kumar, N., Fosso-Kankeu, E., & Ray, S. S. (2019). Efficient removal of Pb(II) and Cd(II) from industrial mine water by a hierarchical MoS<sub>2</sub>/SH-MWCNT nanocomposite. *ACS Omega*, 4(9), 13922–13935. <https://doi.org/10.1021/acsomega.9b01603>
- Hama Aziz, K. H., Mustafa, F. S., Omer, K. M., Hama, S., Hamarawf, R. F., & Rahman, K. O. (2023). Heavy metal pollution in the aquatic environment: Efficient and low-cost removal approaches to eliminate their toxicity: A review. *RSC Advances*, 13(26), 17595–17610. <https://doi.org/10.1039/D3RA00723E>
- He, J., Yang, X., Men, B., & Wang, D. (2016). Interfacial mechanisms of heterogeneous Fenton reactions catalyzed by iron-based materials: A review. *Journal of Environmental Sciences*, 39, 97–109. <https://doi.org/10.1016/j.jes.2015.12.003>
- Hettiarachchi, G. M., Betts, A. R., Chandima Wekumbura, W. G., Lake, L., Mayer, M. M., Scheckel, K. G., & Basta, N. T. (2024). Lead: The most extensively spread toxic environmental contaminant. In R. Naidu (Eds.), *Inorganic contaminants and radionuclides* (pp. 113–150). Elsevier. <https://doi.org/10.1016/B978-0-323-90400-1.00006-9>
- Huang, Y.-H., Hsueh, C.-L., Huang, C.-P., Su, L.-C., & Chen, C.-Y. (2007). Adsorption thermodynamic and kinetic studies of Pb(II) removal from water onto a vermiculite Al<sub>2</sub>O<sub>3</sub>-supported iron oxide. *Separation and Purification Technology*, 55(1), 23–29. <https://doi.org/10.1016/j.seppur.2006.10.023>
- Huang, Z.-H., Zheng, X., Lv, W., Wang, M., Yang, Q.-H., & Kang, F. (2011). Adsorption of lead(II) ions from aqueous solution on low-temperature exfoliated graphene nanosheets. *Langmuir*, 27(12), 7558–7562. <https://doi.org/10.1021/la200606r>
- Hussain, T., Akhter, N., Nadeem, R., Rashid, U., Noreen, S., Anjum, S., Ullah, S., Hussain, H. R., Ashfaq, A., Perveen, S. A., Alharthi, F., & Kazerooni, E. A. (2023). Biogenic synthesis of date stones biochar-based zirconium oxide nanocomposite for the removal of hexavalent chromium from aqueous solution. *Applied Nanoscience*, 13(9), 6053–6066. <https://doi.org/10.1007/s13204-022-02599-z>
- Jaria, G., Calisto, V., Esteves, V. I., & Otero, M. (2022). Overview of relevant economic and environmental aspects of waste-based activated carbons aimed at adsorptive water treatments. *Journal of Cleaner Production*, 344, Article 130984. <https://doi.org/10.1016/j.jclepro.2022.130984>
- Jin, Y., Wang, Y., Li, X., Luo, T., Ma, Y., Wang, B., & Liang, H. (2023). Remediation and its biological responses to Cd(II)-Cr(VI)-Pb(II) multi-contaminated soil by supported nano zero-valent iron composites. *Science of The Total Environment*, 867, Article 161344. <https://doi.org/10.1016/j.scitotenv.2022.161344>
- Kim, S. H., Park, J.-I., Lee, S., An, H.-R., Kim, H., Son, B., Seo, J., Kim, C., Jeong, Y., Choi, K., Jeong, S., & Lee, H. U. (2024). Enhancing adsorption efficiency for environmentally-friendly removal of As(V) and Pb(II) using a biochar-iron oxide composite. *Applied Surface Science*, 667, Article 160348. <https://doi.org/10.1016/j.apsusc.2024.160348>
- Lee, S.-Z., Chang, L., Yang, H.-H., Chen, C.-M., & Liu, M.-C. (1998). Adsorption characteristics of lead onto soils. *Journal of Hazardous Materials*, 63(1), 37–49. [https://doi.org/10.1016/S0304-3894\(98\)00203-9](https://doi.org/10.1016/S0304-3894(98)00203-9)
- Levin, R., Zilli Vieira, C. L., Rosenbaum, M. H., Bischoff, K., Mordarski, D. C., & Brown, M. J. (2021). The urban lead (Pb) burden in humans, animals and the natural environment. *Environmental Research*, 193, Article 110377. <https://doi.org/10.1016/j.envres.2020.110377>
- Liang, X., Wei, G., Xiong, J., Tan, F., He, H., Qu, C., Yin, H., Zhu, J., Zhu, R., Qin, Z., & Zhang, J. (2017). Adsorption isotherm, mechanism, and geometry of Pb(II) on magnetites substituted with transition metals. *Chemical Geology*, 470, 132–140. <https://doi.org/10.1016/j.chemgeo.2017.09.003>
- Liu, X., Ju, Y., Mandzhieva, S., Pinski, D., Minkina, T., Rajput, V. D., Roane, T., Huang, S., Li, Y., Ma, L., Q. Clemens, S., & Rensing, C. (2023). Sporadic Pb accumulation by plants: Influence of soil biogeochemistry, microbial community and physiological mechanisms. *Journal of Hazardous Materials*, 444, Article 130391. <https://doi.org/10.1016/j.jhazmat.2022.130391>
- Lu, Y., He, J., & Luo, G. (2013). An improved synthesis of chitosan bead for Pb(II) adsorption. *Chemical Engineering Journal*, 226, 271–278. <https://doi.org/10.1016/j.cej.2013.04.078>
- Lv, L., Hor, M. P., Su, F., & Zhao, X. S. (2005). Competitive adsorption of Pb<sup>2+</sup>, Cu<sup>2+</sup>, and Cd<sup>2+</sup> ions on microporous titanosilicate ETS-10. *Journal of Colloid and Interface Science*, 287(1), 178–184. <https://doi.org/10.1016/j.jcis.2005.01.073>
- Nassar, N. N. (2010). Rapid removal and recovery of Pb(II) from wastewater by magnetic nanoadsorbents. *Journal of Hazardous Materials*, 184(1–3), 538–546. <https://doi.org/10.1016/j.jhazmat.2010.08.069>
- Nawab, J., Din, Z. U., Ahmad, R., Khan, S., Zafar, M. I., Faisal, S., Raziq, W., Khan, H., Rahman, Z. U., Ali, A., Khan, M. Q., Ullah, S., & Rahman, A. (2021). Occurrence, distribution, and pollution indices of potentially toxic elements within the bed sediments of the riverine system in Pakistan. *Environmental Science and Pollution Research*, 28(39), 54986–55002. <https://doi.org/10.1007/s11356-021-14783-9>
- Nawab, J., Ghani, J., Ullah, S., Ahmad, I., Akbar Jadoon, S., Ali, S., Hamidova, E., Muhammad, A., Waqas, M., Din, Z. U., Khan, S., Khan, A., Ur Rehman, S. A., Javed, T., Luqman, M., & Ullah, Z. (2024). Influence of agro-wastes derived biochar and their composite on reducing the mobility of toxic heavy metals and their bioavailability in industrial contaminated soils. *International Journal of Phytoremediation*. Advance online publication. <https://doi.org/10.1080/15226514.2024.2357640>
- Nawab, J., Idress, M., Ullah, S., Rukh, G., Zainab, R., Sher, H., Ghani, J., Khan, S., Ullah, Z., Ahmad, I., & Ali, S. W. (2023). Occurrence and distribution of heavy metals in mining degraded soil and medicinal plants: A case study of Pb/Zn sulfide terrain Northern Areas, Pakistan. *Bulletin of Environmental Contamination and Toxicology*, 110(1), Article 24. <https://doi.org/10.1007/s00128-022-03673-6>
- Noman, M., Haziq, M. A., Safi, B. U., Ullah, S., Rukh, G., Faiq, M. E., Ullah, Z., Bibi, S. D., Shaukat, S., Emiliya, H., Rahim, Z., Ali, K. S., Khan, F., & Can, W. (2022). Lead (II) adsorption from aqueous systems using visible light activated cobalt doped zinc oxide nanoparticles. *Digest Journal of Nanomaterials and Biostructures*, 17(3), 838–849. <https://doi.org/10.15251/DJNB.2022.173.839>
- Oladoye, P. O. (2022). Natural, low-cost adsorbents for toxic Pb(II) ion sequestration from (waste)water: A state-of-the-art review. *Chemosphere*, 287, Article 132130. <https://doi.org/10.1016/j.chemosphere.2021.132130>
- Pal, P., Edathil, A. A., Chaurasia, L., Rambabu, K., & Banat, F. (2018). Removal of sulfide from aqueous solutions using novel alginate-iron oxide magnetic hydrogel composites. *Polymer Bulletin*, 75(12), 5455–5475. <https://doi.org/10.1007/s00289-018-2338-6>
- Prasad, P. S., Gomathi, T., Sudha, P. N., Deepa, M., Rambabu, K., & Banat, F. (2022). Biosilica/Silk Fibroin/Polyurethane biocomposite for toxic heavy metals removal

- from aqueous streams. *Environmental Technology & Innovation*, 28, Article 102741. <https://doi.org/10.1016/j.eti.2022.102741>
- Raj, K., & Das, A. P. (2023). Lead pollution: Impact on environment and human health and approach for a sustainable solution. *Environmental Chemistry and Ecotoxicology*, 5, 79–85. <https://doi.org/10.1016/j.enccoco.2023.02.001>
- Rambabu, K., AlYammahi, J., Bharath, G., Thanigaivelan, A., Sivarajasekar, N., & Banat, F. (2021). Nano-activated carbon derived from date palm coir waste for efficient sequestration of noxious 2,4-dichlorophenoxyacetic acid herbicide. *Chemosphere*, 282, Article 131103. <https://doi.org/10.1016/j.chemosphere.2021.131103>
- Rambabu, K., Banat, F., Nirmala, G. S., Velu, S., Monash, P., & Arthanareeswaran, G. (2019). Activated carbon from date seeds for chromium removal in aqueous solution. *Desalination and Water Treatment*, 156, 267–277. <https://doi.org/10.5004/dwt.2018.23265>
- Rambabu, K., Bharath, G., Avornyo, A., Thanigaivelan, A., Hai, A., & Banat, F. (2023). Valorization of date palm leaves for adsorptive remediation of 2,4-dichlorophenoxyacetic acid herbicide polluted agricultural runoff. *Environmental Pollution*, 316, Article 120612. <https://doi.org/10.1016/j.envpol.2022.120612>
- Rambabu, K., Thanigaivelan, A., Bharath, G., Sivarajasekar, N., Banat, F., & Show, P. L. (2021). Biosorption potential of Phoenix dactylifera coir wastes for toxic hexavalent chromium sequestration. *Chemosphere*, 268, Article 128809. <https://doi.org/10.1016/j.chemosphere.2020.128809>
- Rodda, D. P., Johnson, B. B., & Wells, J. D. (1996). Modeling the effect of temperature on adsorption of Lead(II) and Zinc(II) onto goethite at constant pH. *Journal of Colloid and Interface Science*, 184(2), 365–377. <https://doi.org/10.1006/jcis.1996.0631>
- Shaukat, S., Hassani, M. A., Yadgari, M. Y., Ullah, S., Iqbal, M. S., Khan, F., Bibi, S. D., Ullah, Z., Hassani, M. A., Rukh, G., Sabir, M., Hussain, S. A., Arshad, N., Ali, S., Izhar, S. K., & Afsar, S. (2022). Green synthesis of silver nanoparticles and its application towards As(V) removal from aqueous systems. *Digest Journal of Nanomaterials and Biostructures*, 17(4), 1385–1398. <https://doi.org/10.15251/DJNB.2022.174.1385>
- Sun, H., Zhang, X., Niu, Q., Chen, Y., & Crittenden, J. C. (2007). Enhanced accumulation of arsenate in carp in the presence of titanium dioxide nanoparticles. *Water, Air, and Soil Pollution*, 178(1–4), 245–254. <https://doi.org/10.1007/s11270-006-9194-y>
- Tabesh, S., Davar, F., & Loghman-Estarki, M. R. (2018). Preparation of  $\gamma$ -Al<sub>2</sub>O<sub>3</sub> nanoparticles using modified sol-gel method and its use for the adsorption of lead and cadmium ions. *Journal of Alloys and Compounds*, 730, 441–449. <https://doi.org/10.1016/j.jallcom.2017.09.246>
- Tarekegn, M. M., Hiruy, A. M., & Dekebo, A. H. (2021). Nano zero valent iron (nZVI) particles for the removal of heavy metals (Cd<sup>2+</sup>, Cu<sup>2+</sup> and Pb<sup>2+</sup>) from aqueous solutions. *RSC Advances*, 11(30), 18539–18551. <https://doi.org/10.1039/D1RA01427G>
- Tee, G. T., Gok, X. Y., & Yong, W. F. (2022). Adsorption of pollutants in wastewater via biosorbents, nanoparticles and magnetic biosorbents: A review. *Environmental Research*, 212, Article 113248. <https://doi.org/10.1016/j.envres.2022.113248>
- Tholley, M. S., George, L. Y., Wang, G., Ullah, S., Qiao, Z., Ling, S., Wu, J., Peng, C., & Zhang, W. (2023). Risk assessment and source apportionment of heavy metalloids from typical farmlands provinces in China. *Process Safety and Environmental Protection*, 171, 109–118. <https://doi.org/10.1016/j.psep.2022.12.092>
- Uheida, A., Iglesias, M., Fontàs, C., Hidalgo, M., Salvadó, V., Zhang, Y., & Muhammed, M. (2006). Sorption of palladium(II), rhodium(III), and platinum(IV) on Fe<sub>3</sub>O<sub>4</sub> nanoparticles. *Journal of Colloid and Interface Science*, 301(2), 402–408. <https://doi.org/10.1016/j.jcis.2006.05.015>
- Ullah, S., Hayat, K., & Qiao, X. (2023). Chitosan-based biostimulation: A novel approach for simultaneous remediation of co-existing cadmium and arsenic contamination in soil. *Air, Soil and Water Research*, 16, 1–13. <https://doi.org/10.1177/11786221231216862>
- Ullah, S., Shams, D. F., Ur Rehman, S. A., Khattak, S. A., Noman, M., Rukh, G., Bibi, H., Ateeq, M., Bibi, N., Ali, L., & Fazil, P. (2022). Application of visible light activated thiolated cobalt doped ZnO nanoparticles towards arsenic removal from aqueous systems. *Digest Journal of Nanomaterials and Biostructures*, 17(2), 443–455. <https://doi.org/10.15251/DJNB.2022.172.443>
- Wang, T., Liu, W., Xiong, L., Xu, N., & Ni, J. (2013). Influence of pH, ionic strength and humic acid on competitive adsorption of Pb(II), Cd(II) and Cr(III) onto titanate nanotubes. *Chemical Engineering Journal*, 215–216, 366–374. <https://doi.org/10.1016/j.cej.2012.11.029>
- Xiao, S., Cheng, M., Zhong, H., Liu, Z., Liu, Y., Yang, X., & Liang, Q. (2020). Iron-mediated activation of persulfate and peroxymonosulfate in both homogeneous and heterogeneous ways: A review. *Chemical Engineering Journal*, 384, Article 123265. <https://doi.org/10.1016/j.cej.2019.123265>
- Xie, P., Zahoor, F., Iqbal, S. S., Zahoor, Ullah, S., Noman, M., Din, Z. U., & Yang, W. (2022). Elimination of toxic heavy metals from industrial polluted water by using hydrophytes. *Journal of Cleaner Production*, 352, Article 131358. <https://doi.org/10.1016/j.jclepro.2022.131358>
- Xiong, C., Xue, C., Huang, L., Hu, P., Fan, P., Wang, S., Zhou, X., Yang, Z., Wang, Y., & Ji, H. (2021). Enhanced selective removal of Pb(II) by modification low-cost bio-sorbent: Experiment and theoretical calculations. *Journal of Cleaner Production*, 316, Article 128372. <https://doi.org/10.1016/j.jclepro.2021.128372>
- Xu, R., Tang, C., & Liu, M. (2020). A novel nitrified aerobic granular sludge biosorbent for Pb(II) removal: Behaviors and mechanisms. *Journal of Dispersion Science and Technology*, 41(14), 2223–2231. <https://doi.org/10.1080/01932691.2019.1656641>
- Yadgari, M. Y., Subat, S., Rashid, S., Ullah, S., Li, L., Hassani, M. A., Emiliya, H., & Rukh, G. (2023). Toxic effects of arsenic and its adsorption through thiolated cobalt doped silver nanomaterials from water resources. *Digest Journal of Nanomaterials and Biostructures*, 18(4), 1339–1350. <https://doi.org/10.15251/DJNB.2023.184.1339>
- Yang, S., Zhao, D., Zhang, H., Lu, S., Chen, L., & Yu, X. (2010). Impact of environmental conditions on the sorption behavior of Pb(II) in Na-bentonite suspensions. *Journal of Hazardous Materials*, 183(1–3), 632–640. <https://doi.org/10.1016/j.jhazmat.2010.07.072>
- Yang, Z., Hou, J., Wu, J., & Miao, L. (2021). The effect of carbonization temperature on the capacity and mechanisms of Pb(II) adsorption by microalgae residue-derived biochar. *Ecotoxicology and Environmental Safety*, 225, Article 112750. <https://doi.org/10.1016/j.ecoenv.2021.112750>
- Zannotti, M., Piras, S., Remia, L., Appignanesi, D., & Giovannetti, R. (2024). Selective colorimetric detection of Pb(II) ions by using green synthesized gold nanoparticles with orange peel extract. *Chemosensors*, 12(3), Article 33. <https://doi.org/10.3390/chemosensors12030033>
- Zhang, Z., Wang, T., Zhang, H., Liu, Y., & Xing, B. (2021). Adsorption of Pb(II) and Cd(II) by magnetic activated carbon and its mechanism. *Science of The Total Environment*, 757, Article 143910. <https://doi.org/10.1016/j.scitotenv.2020.143910>